Linked Thermal and Solute Perturbation Analysis of Cooperative Domain Interactions in Proteins. Structural Stability of Diphtheria Toxin†

Glen Ramsay and Ernesto Freire*

Department of Biology, Biocalorimetry Center, The Johns Hopkins University, Baltimore, Maryland 21218

Received May 8, 1990; Revised Manuscript Received June 22, 1990

ABSTRACT: The temperature and guanidine hydrochloride (GuHCl) dependence of the structural stability of diphtheria toxin has been investigated by high-sensitivity differential scanning calorimetry. In 50 mM phosphate buffer at pH 8.0 and in the absence of GuHCl, the thermal unfolding of diphtheria toxin is characterized by a transition temperature (T_m) of 54.9 °C, a calorimetric enthalpy change (ΔH) of 295 kcal/mol, and a van't Hoff to calorimetric enthalpy ratio of 0.57. Increasing the GuHCl concentration lowers the transition temperature and the calorimetric enthalpy change. At the same time, the van't Hoff to calorimetric enthalpy ratio increases until it reaches a value of 1 at 0.3 M GuHCl and remains constant thereafter. At low GuHCl concentrations (0–0.3 M), the thermal unfolding of diphtheria toxin is characterized by the presence of two transitions corresponding to the A and B domains of the protein. At higher GuHCl concentrations (0.3–1 M), the A domain is unfolded at all temperatures, and only one transition corresponding to the B domain is observed. Under these conditions, the most stable protein conformation at low temperatures is a partially folded state in which the A domain is unfolded and the B domain folded. A general model that explicitly considers the energetics of domain interactions has been developed in order to account for the stability and cooperative behavior of diphtheria toxin. It is shown that this cooperative domain interaction model correctly accounts for the temperature location as well as the shape and area of the calorimetric curves. Under physiological conditions, domain–domain interactions account for most of the structural stability of the A domain. At 37 °C, the free energy of stabilization of the isolated A domain is only −2.2 kcal/mol. Domain–domain interactions contribute an extra −2.5 kcal/mol to the stabilization of the A subunit. Further linkage of the conformational and binding equilibrium equations has allowed us to develop a multidimensional deconvolution procedure and model the entire temperature–GuHCl stability surface of the protein. This analysis has permitted a more thorough characterization of the partially unfolded intermediate believed to exist during the membrane translocation of the toxin A fragment.

Diphtheria toxin (DT) is a protein with the ability to exist in both water-soluble and membrane-associated states. It is secreted in water-soluble form by *Corynebacterium diphtheriae* as a single polypeptide chain with a molecular weight of 58 342. It is structurally composed of two domains (A, M_r = 21 100; and B, M_r = 37 200) which after secretion are proteolytically nicked but remain associated via a disulfide bond (DeLange et al., 1979; Drazin et al., 1979; Falmagne et al., 1985). Reduction of the disulfide bridge yields two fragments, one of which, the A fragment, is capable of catalyzing the ADP-ribosylation and inactivation of elongation factor II, resulting in the inhibition of protein synthesis. The initial step of cytotoxicity by diphtheria toxin is the binding of the toxin to a cell surface receptor (Proia et al., 1979; Hranitzky et al., 1985; Cieplak et al., 1987). The toxin is then endocytosed, where it is exposed to a pH of approximately 5 (Ohkuma & Poole, 1978; Jensen & Bainton, 1973). The exposure of the toxin to an acidic environment is thought to provide the driving force for the insertion of the toxin into the membrane and the translocation of the A domain into the cytosol. Following toxin insertion and translocation of the A domain, the disulfide bond is reduced on the cytosolic side of the membrane (Moskaug et al., 1987), and the A fragment is released into the cytosol. In vitro studies have shown that exposure of the toxin to a low pH triggers a conformational change which results in increased hydrophobicity of the toxin (Sandvig & Olsnes, 1981; Blewitt et al., 1984). Recently, a systematic thermodynamic characterization of the thermal and pH stabilities of diphtheria toxin by high-sensitivity differential scanning calorimetry (Ramsay et al., 1989) revealed that the pH-induced change in conformation corresponds to the unfolding of the toxin molecule. Also, these studies suggested that the thermal unfolding of the toxin can be well represented as a sum of two two-state transitions corresponding to the A and B domains (Ramsay et al., 1989).

Folding/unfolding transitions in multidomain proteins are usually characterized by the presence of several cooperative transitions. When studied by differential scanning calorimetry, these transitions give rise to multiple, sometimes strongly overlapped peaks. Even though the fundamental theory for the deconvolution of these transitions was developed in a rigorous way several years ago (Freire & Biltonen, 1978), it is sometimes experimentally difficult to deduce unique transition mechanisms and domain stability thermodynamics due to statistical correlations between transition parameters. In this paper, we present a general model for cooperative domain interactions and show that the protein conformational equilibrium can be linked to ligand binding equations in order to define three-dimensional protein stability surfaces. Multidimensional deconvolution of the experimental heat capacity surface then allows a precise characterization of the transition mechanism of multidomain proteins. The results of this analysis have been applied to the unfolding transition of diphtheria toxin and its dependence on guanidine hydrochloride

† Supported by grants from the National Institutes of Health (GM 37911 and RR 04328).

* To whom correspondence should be addressed.

0006-2960/90/0429-8677$02.50/0

(GuHCl) concentration. The rationale for this approach is that different structural domains of a protein may interact with ligands differently, thus allowing manipulation of the distribution of protein states by the addition of such ligands. The combined use of thermal and GuHCl perturbations to measure changes in protein stability allows a more rigorous and statistically robust definition of thermodynamic parameters than is possible by the two perturbations used independently. In this paper, we have examined the combined effects of temperature, and GuHCl on the thermodynamic stability of diphtheria toxin.

Materials and Methods

Toxin Purification. Crude diphtheria toxin (lot D693) was purchased from Connaught Laboratories Ltd., Willowdale, Canada, and purified by HPLC using a TSK DEAE-5PW (LKB) ion-exchange column followed by molecular sieve chromatography as described before (Collier & Kandel, 1971; Ramsay et al., 1989). Diphtheria toxin purified by this method yielded better than 90% nicked monomer. Impurities consisted mainly of unnicked toxin and proteolytic fragments of toxin. The nicked monomer consisted of a native mixture of nucleotide-free and bound toxin species. The relative amounts of nucleotide-free and nucleotide-bound species varied from lot to lot, but were in the range of 50–90% nucleotide-bound.

Separation of Nucleotide-Free and -Bound Toxin Species. After being dialyzed 3 times against Tricine buffer, the crude toxin was passed through a 0.22-μm membrane filter and loaded onto a matrex Green A (Amicon Corp., Lexington, MA) column (1.8 × 20 cm) at a flow rate of 0.07 mL/min. The column was rinsed with Tricine buffer until the nucleotide-bound toxin and impurities had passed through; then Tricine buffer containing 0.75 M NaCl was used to elute the nucleotide-free toxin. The nucleotide-free and -bound fractions were pooled separately and concentrated by ammonium sulfate precipitation. The toxin species were resuspended and dialyzed, and monomeric toxin was obtained by molecular sieve chromatography as described for the purification of toxin containing a native mixture of species. The nucleotide-bound and -free species obtained were 99% pure nicked, monomeric toxin as judged by SDS gel electrophoresis. For the experiments described in this paper, only nucleotide-bound, nicked, diphtheria toxin was used.

Polyacrylamide Gel Electrophoresis. Toxin purity was checked by discontinuous sodium dodecyl sulfate (SDS)–polyacrylamide gel electrophoresis (PAGE) with a 3% stacking gel (pH 6.8) and a 10% running gel (pH 8.8). Samples were prepared by mixing 20 μL of protein with 20 μL of 17% sucrose, 0.17% phenol red, and 1 M Tris (pH 8.8) (sucrose solution) and 20 μL of 1.7 M urea and 3% SDS (denaturing solution) (3% β-mercaptoethanol was included in the denaturing solution for reducing gels). This mixture was boiled for 2 min, and 55 μL was loaded onto the gel. The gels were ran at 8 mA until the dye front had entered the running gel; then the current was set at 15 mA until the dye front had reached the bottom of the gel, at which time the run was stopped. The gel was stained overnight using Coomasie blue (10% v/v acetic acid, 40% H_2O, 50% methanol, and 0.2% w/v Coomasie brilliant blue-R) and destained (10% acetic acid, 10% methanol, and 80% H_2O). Native gels were prepared by the same protocol as for SDS–PAGE, except that water was substituted for concentrated SDS. The running and staining conditions were the same as for SDS gels.

Differential Scanning Calorimetry. All calorimetric scans were performed with a Microcal MC-2 differential scanning calorimeter. The calorimetric unit was interfaced to an IBM PC microcomputer using an A/D converter board (Data Translation DT-2801) for automatic data collection and analysis. A scan rate of 60 °C/h was used in all experiments. Protein concentrations were determined after each scan (Lowry et al., 1951; Collier & Kandel, 1971) and were on the order of 1 mg/mL. The calorimetric scans were performed in 50 mM PO_4 and 0.01% NaN_3, pH 8.0 (phosphate buffer), containing different concentrations of GuHCl. A 4 M GuHCl stock solution was made by lyophilizing GuHCl crystals (grade 1, Sigma Chemical Co., St. Louis, MO) overnight and dissolving the dried crystals in phosphate buffer the next day. This method gives accurate results as checked by refractive index measurements. Samples to be scanned in the calorimeter were prepared by mixing stock DT with phosphate buffer and stock GuHCl solution to make a 1 mg/mL protein solution containing the desired GuHCl concentration. The pH of all buffer solutions was checked immediately prior the calorimetric scans.

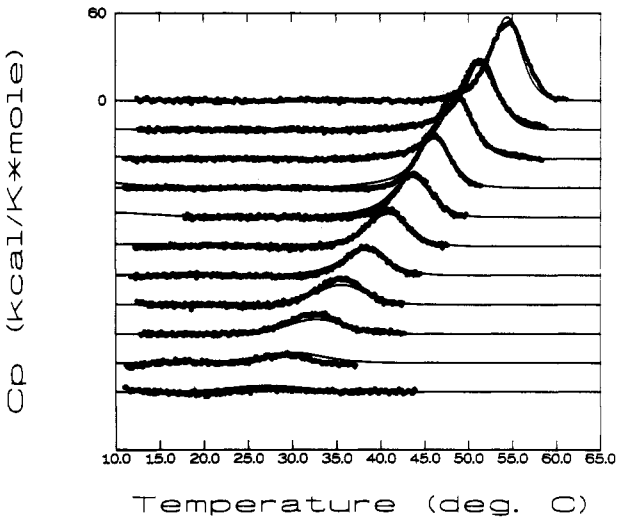

FIGURE 1: Excess heat capacity function versus temperature for diphtheria toxin (DT) in 50 mM sodium phosphate buffer, pH 8.0, and increasing concentrations of GuHCl. From top to bottom, the GuHCl molar concentrations are 0, 0.1, 0.2, 0.3, 0.4, 0.5, 0.6, 0.7, 0.8, 0.9, and 1.0. The curves have been shifted in the y axis for display purposes. The circles represent the experimental points and the solid lines the theoretical curves predicted by the cooperative model developed in this paper.

Data Analysis. All the data analysis in this paper was performed on a Hewlett-Packard 835 Turbo SRX superminicomputer. Nonlinear least-squares analysis was performed by using the Marquardt (Marquardt, 1963) and the Simplex minimization algorithms (Nelder & Mead, 1965) using software developed in this laboratory (Masserini & Freire, 1988).

Results and Discussion

High-Sensitivity Differential Scanning Calorimetry. The thermal stability of DT was measured at different GuHCl concentrations by high-sensitivity differential scanning calorimetry. The resulting excess heat capacity (C_p) versus temperature profiles for DT at increasing concentrations of GuHCl are shown in Figure 1. The increase in the concentration of GuHCl from 0 to 1 M is accompanied by a monotonic decrease in the transition temperature, T_m, defined as the temperature location of the maximum in the excess heat capacity function. Under the conditions of these experiments, T_m is equal to 54.9 °C at zero GuHCl concentration and decreases to 27.3 °C at 1 M GuHCl. This is the expected effect of a denaturant on the structural stability of a protein. Furthermore, a decrease in the measured enthalpy is also observed.

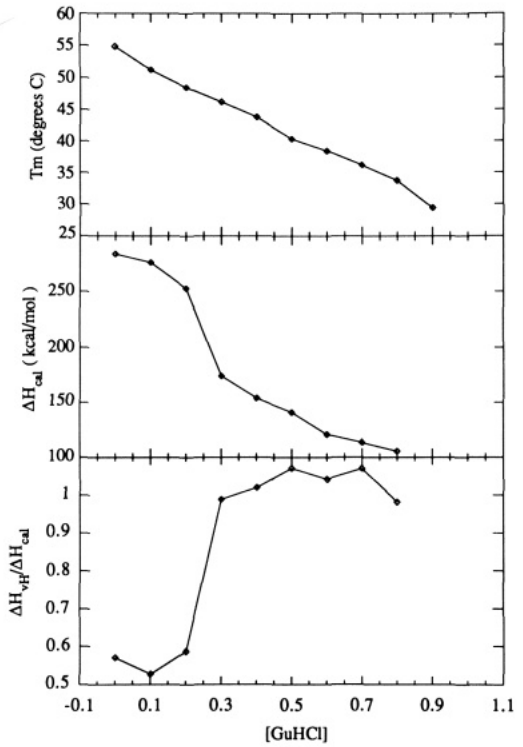

FIGURE 2: Dependence of overall thermodynamic parameters for diphtheria toxin unfolding as a function of the molar concentration of GuHCl.

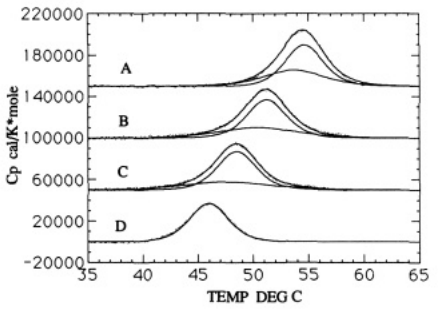

FIGURE 3: Deconvolution of DT excess heat capacity curves obtained at 0, 0.1, 0.2, and 0.3 M GuHCl. The experimental data are represented by dots and the theoretical curves by solid lines. Note that at 0.3 M GuHCl the amplitude of the low-enthalpy transition is almost negligible.

At zero GuHCl, the enthalpy change is 295 kcal/mol whereas at 1 M GuHCl the enthalpy of the transition is only 40 kcal/mol. Figure 2 summarizes the dependence of the measured thermodynamic parameters (T_m, ΔH, and $\Delta H_{vH}/\Delta H$) on GuHCl concentration. Analysis of the enthalpy for the entire transition process versus GuHCl concentration reveals that the calorimetric ΔH decreases in a sigmoidal fashion with an inflection point centered around 0.3 M GuHCl. Up to a GuHCl concentration of 0.3 M, the van't Hoff enthalpy, ΔH_{vH}, is smaller than the calorimetric enthalpy, indicating that the unfolding process involves multiple transition steps. At higher GuHCl concentrations, the calorimetric and van't Hoff enthalpies are approximately equal, indicating that under these conditions the transition becomes a two-state transition.

Judging by the ratios of the van't Hoff to calorimetric enthalpies, the unfolding of DT involves more than a single two-state transition at low GuHCl concentrations. Deconvolution analysis of the excess heat capacity profiles (Freire & Biltonen, 1978; Freire, 1989) obtained under those conditions indicates that the entire transition can be well described by the sum of two two-state transitions as shown in Figure 3.

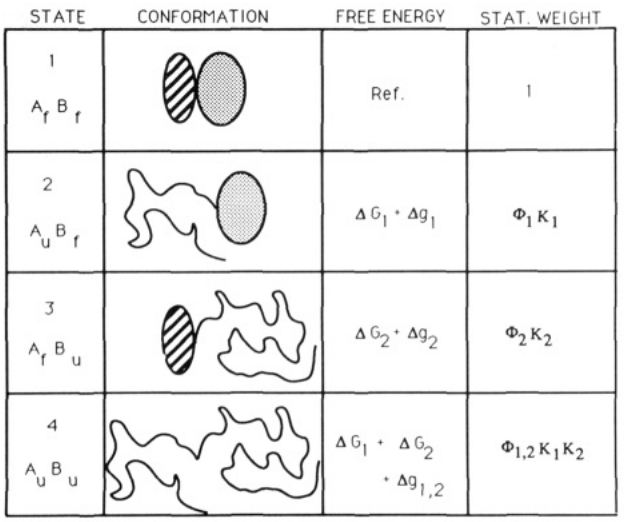

FIGURE 4: Schematic representation of the four different states associated with the folding/unfolding transition of a protein consisting of two cooperative folding units. The statistical weights are defined in terms of the intrinsic free energies (ΔG's) and interaction free energies (Δg's) as follows: $K_i = \exp(-\Delta G_i/RT)$ and $\Phi_i = \exp(-\Delta g_i/RT)$ where T is the absolute temperature and R the gas constant.

At zero GuHCl concentration, the enthalpies of these two transitions are 184 and 110 kcal/mol, respectively. On the basis of experiments performed with the isolated A fragment, we have previously assigned the low-enthalpy transition to the A domain and the high-temperature transition to the B domain. It must be noted that in this case the enthalpy values are also proportional to the molecular weights of the A and B domains. As shown in Figure 3, the area corresponding to the high enthalpy transition (B transition) exhibits only a slight decrease up to 0.3 M GuHCl even though its transition temperature decreases from 54.9 to 46.0 °C. On the other hand, the area of the low-enthalpy transition (A transition) decreases dramatically and disappears almost completely at 0.3 M GuHCl. Under these conditions, the A domain presumably exists in the unfolded state at all temperatures, and the transition observed calorimetrically becomes a two-state transition corresponding to the unfolding of the B domain.

Cooperative Domain Interactions. The thermal unfolding of multidomain proteins is often characterized by $\Delta H_{vH}/\Delta H$ ratios smaller than unity, indicating that the folding/unfolding transition involves the presence of thermodynamically stable partially unfolded states (Biltonen & Freire, 1978; Privalov, 1979, 1982). If this is the case, the excess heat capacity function is composed of multiple transition peaks, independently of whether they are well separated or completely overlapped in the temperature scale. These peaks define cooperative units within the protein, i.e., structural elements whose folding/unfolding process is thermodynamically described by an elementary two-state transition. In most proteins, the number of cooperative folding units is usually less than the number of structural domains due to the existence of strong cooperative interactions between two or more domains. These cooperative interactions couple the folding/unfolding of those domains in such a way that they behave as single cooperative units. As a result, the number of cooperative folding units is usually equal or less than the number of structural domains. This behavior has been observed for several proteins [see, for example, Privalov and Khechinashvili (1974), Privalov (1982), Ghelis and Yon (1982), and Creighton (1984)].

For the case of a two-domain protein, there are four different states as indicated in Figure 4. From a statistical thermodynamic point of view, it is possible to define the Gibbs free

energies and statistical weights for each conformational state as indicated in Figure 4. This formalism considers explicitly interdomain interactions for the completely folded (A_fB_f), partially folded (A_uB_f and A_fB_u), and completely unfolded (A_uB_u) states in addition to the intrinsic free energies of stabilization for each domain. The interaction terms may arise from different sources including domain–domain as well as domain–solvent interactions. For example, partially unfolded states not only loose folded domain interactions existing in the native state but also may gain new interactions resulting from the exposure to the solvent of previously buried regions or even interactions between the unfolded and folded domains. According to these definitions, the partition function for the conformational equilibrium can be written as

$$Q = 1 + \Phi_1 K_1 + \Phi_2 K_2 + \Phi_{1,2} K_1 K_2 \quad (1)$$

where the Φ terms correspond to the various interdomain interactions and the K terms to the intrinsic stability constants per domain. The term $\Phi_{1,2}$ has been included explicitly for completeness. In general, it will differ from unity only in the case in which "domain–domain" interactions are also present in the unfolded state. Previously, Brandts et al. (1989) have presented a model in which only interactions in the completely folded state are taken into consideration. Mathematically, that model is a particular case of the general model presented here and is also described by eq 1 when $\Phi_1 = \Phi_2 = \Phi_{1,2}$. The average excess enthalpy, $\langle \Delta H \rangle$ can be expressed in terms of the population of each state, P_i, as:

$$\langle \Delta H \rangle = \sum \Delta H_i P_i = [\Delta H_1 \Phi_1 K_1 + \Delta H_2 \Phi_2 K_2 + (\Delta H_1 + \Delta H_2) \Phi_{1,2} K_1 K_2]/Q \quad (2)$$

The above equation assumes that the interdomain interaction enthalpy is very small compared to the overall stabilization enthalpy. The heat capacity function measured by differential scanning calorimetry is the temperature derivative of the excess enthalpy function and is calculated directly from eq 2:

$$C_p = \mathrm{d}\langle \Delta H \rangle / \mathrm{d}T = \sum \Delta H_i \, \mathrm{d}P_i/\mathrm{d}T + \sum P_i \, \mathrm{d}\Delta H_i/\mathrm{d}T \quad (3)$$

In the above equation, the first term on the right-hand side gives rise to the characteristic peaks associated with thermally induced transitions whereas the second term on the right-hand side gives rise to the sigmoidal base-line shift observed in transitions exhibiting a ΔC_p. This sigmoidal base line can be subtracted from the experimental data in order to obtain an excess heat capacity function described only by the first term on the right-hand side of eq 3 as discussed previously by Freire (1989) and also by Shriver and Kamath (1990). It should be noted that the $\Delta C_{p,i}$ terms are still included in the equation and therefore in the analysis procedure.

The resulting equation for the excess heat capacity function was used in the analysis of the experimental data. Previously, we have measured the thermal unfolding of the isolated A fragment of the toxin and show that it is a reversible two-state transition characterized by a T_m of 44.2 °C and a ΔH of 89 kcal/mol at that temperature (Ramsay et al., 1989). The interaction with the B domain in the intact toxin increases the T_m of the A domain to 54 °C, consistent with an additional free energy of stabilization of −2.6 kcal/mol at that temperature. Also, at 54 °C, the enthalpy change for the A domain increases to about 100–120 kcal/mol as a result of the ΔC_p for the transition. The experimental values obtained independently for the isolated A domain were used in the analysis of the heat capacity profile for the intact toxin in order to fit for the unknown parameters by nonlinear least-squares

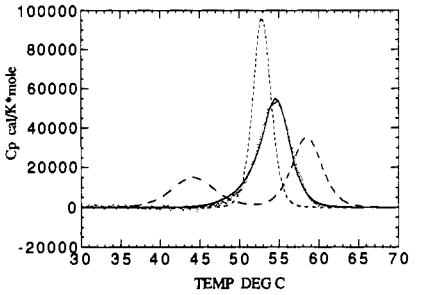

FIGURE 5: Experimental (dots) and theoretical (solid line) excess heat capacity curve for diphtheria toxin in the absence of GuHCl. The theoretical solid curve was calculated with the model developed in this paper and the parameters summarized in Table I. The long dashed curve (– –) represents the expected curve for the case in which the two domains behave independently of each other and the short dashed curve (- - -) the expected curve for the case in the two domains behave as a single cooperative unit.

Table I: Energetics of Domain Stabilization for Diphtheria Toxin[a]

domain	T_m^0 (°C)	ΔH (kcal/mol)	Φ
(1) A	44.2 ± 0.2	110 ± 10	0.03 ± 0.01
(2) B	58.9 ± 1.2	175 ± 15	0

[a] The intrinsic parameters for the A domain (T_m^0 and ΔH) were estimated independently from experiments with the isolated fragment. The term $\Phi_{1,2}$ is set equal to 1 as discussed in the text.

analysis. The results of this analysis are shown in Figure 5 where the experimental and predicted heat capacity profiles have been plotted as a function of temperature. The energetic parameters that best fit the data are shown in Table I. It is clear that the partition function in eq 1 correctly predicts the transition temperatures as well as the shape of the calorimetric profile. For comparison, Figure 5 also shows the expected calorimetric profile for the case in which the interaction terms Φ_1 and Φ_2 are set equal to 1 (two independent domains) and for the case in which they are equal to 0 (infinitely cooperative domains resulting in overall two-state transition). According to the results of this analysis, the A domain is stabilized by its interaction with the B domain by an additional −2.5 ± 0.3 kcal/mol, in close agreement with the results obtained previously by van't Hoff analysis (Ramsay et al., 1989). On the other hand, the zero value obtained for the cooperative term Φ_2 indicates that the state in which the A domain is folded and the B domain unfolded (A_fB_u) never becomes populated within the limits of detection of these experiments.

The major importance of the above formalism is its ability to predict the correct shape of the heat capacity function for the intact toxin. As discussed previously (Freire & Biltonen, 1978), the shape of the heat capacity function associated with a transition directly reflects the transition mechanism. According to the predicted transition mechanism for diphtheria toxin, the unfolding of the molecule involves only one significantly populated intermediate corresponding to the state in which the A domain is already unfolded and the B domain still retains its folded structure (A_uB_f). This result is illustrated in Figure 6 where the population of the various states shown in Figure 4 (top panel) has been plotted as a function of temperature. As expected, the population of the native state decreases to zero as the temperature increases, whereas the population of the intermediate A_uB_f increases and reaches a maximum of 0.5 around 54 °C before decaying to zero as the population of the completely unfolded state A_uB_u reaches its maximal value of unity.

Linkage Analysis. The effect of a ligand on the thermal stability of a protein can be considered explicitly by linking the conformational equilibrium to the binding equilibrium as

Table II: Results of Global Analysis of Heat Capacity Surface

domain	T_m^0 (°C)	ΔH^a (kcal/mol)	ΔC_p [kcal/(K·mol)]	ΔH_b^b (kcal/mol)	ΔS_b^b [cal/(K·mol)]	Δn
A	44.2 ± 0.2[c]	110 ± 15	3.5 ± 2.0	−0.8 ± 0.4	−2.8 ± 1.4	20 ± 10
B	57.9 ± 0.5	190 ± 20	4.3 ± 1.2	−0.8 ± 0.4	−2.8 ± 1.4	51 ± 5

[a] The ΔH values in the table are those at 55 °C, the transition temperature of the toxin in the absence of GuHCl. The ΔH values at any other temperature can be calculated with the standard $\Delta H(T) = \Delta H + \Delta C_p(T - 55)$. [b] ΔH_b and ΔS_b are the enthalpy and entropy of GuHCl binding, respectively. [c] The errors quoted in the table correspond to the parameter variation that results in a change of two standard deviations in the goodness of the fit.

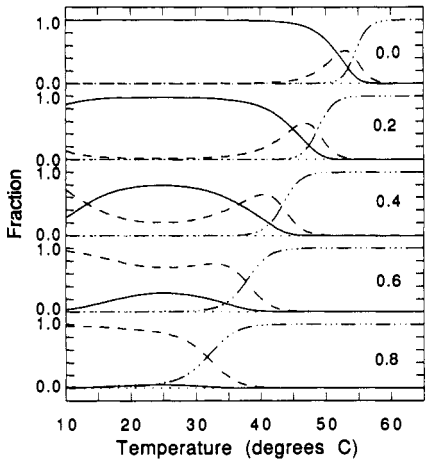

FIGURE 6: Population of states as a function of temperature for diphtheria toxin in the absence of GuHCl (top panel) and in the presence of 0.2, 0.4, 0.6, and 0.8 M GuHCl from top to bottom, respectively. In this figure, the solid line (—) represents the folded state A_fB_f, the dashed line (- - -) the partially unfolded state A_uB_f, the dotted line (···) the A_fB_u state, and the dashed–dotted line (–···–) the unfolded state A_uB_u. Note that the state in which the A domain is unfolded and the B domain remains folded (A_uB_f) is the only partially folded conformation that becomes significantly populated during the course of the transition.

described originally by Wyman (1964). The conformational equilibrium for a cooperative folding unit can be written as

$$F \overset{K^0}{\leftrightarrow} U \tag{4}$$

If each conformation is assumed to have n_f and n_u binding sites for a ligand with intrinsic association constants $K_{b,f}$ and $K_{b,u}$, respectively, then in the presence of the ligand the conformational equilibrium constant is given by

$$K = K^0 \frac{(1 + K_{b,u}[X])^{n_u}}{(1 + K_{b,f}[X])^{n_f}} \tag{5}$$

where K^0 is the equilibrium constant in the absence of the ligand and [X] the free concentration or activity of the ligand. The above equation can be written in a general form for the case of multiple independent binding sites as

$$K = K^0 \frac{\Pi(1 + K_{b,u,i}[X])^{n_{u,i}}}{\Pi(1 + K_{b,f,i}[X])^{n_{f,i}}} \tag{6}$$

where the multiplication runs over all sets of binding sites ($n_{s,u}$ and $n_{s,f}$) for each conformation. $n_{u,i}$ is the number of binding sites with association constant $K_{b,u,i}$ in the U conformation. A similar set of definitions applies to the F conformation.

The interaction of GuHCl with proteins has been extensively studied for many years [see Pace (1986) for a review]. Aune and Tanford (1969a,b) proposed the denaturant binding model to describe GuHCl-induced protein denaturation. According to this model, the folded and unfolded states are assumed to posses multiple, independent binding sites for the denaturant. The binding affinity of GuHCl [or more properly the GuH^+ ions (Castellino & Barker, 1968; Ghelis & Yon, 1982)] to a number of different proteins is rather weak and in the range of 0.1–1.2 M^{-1} (Pfeil, 1981) for both the folded and unfolded states. If it is assumed that the intrinsic binding constant per site is the same in the folded and unfolded states [see Pace (1986)], then the conformational equilibrium constant in the presence of GuHCl (eq 5) becomes

$$K = K^0(1 + k_b a)^{\Delta n} \tag{7}$$

where K^0 is the equilibrium constant in the absence of GuHCl, k_b is the average association constant for GuH^+ ions, and Δn is the difference in the number of GuH^+ binding sites between the unfolded and folded states, also called the preferential interaction parameter. a is the mean ion activity of GuHCl and can be expressed in terms of the GuHCl molarity as described by Pace and Vanderburg (1979):

$$a = 0.6761M - 0.1468M^2 + 0.02475M^3 - 0.001318M^4 \tag{8}$$

According to eq 7, the GuHCl-induced destabilization of the folded conformation is due to the existence of a larger number of binding sites in the unfolded conformation. Presumably, many potential binding sites are not accessible to denaturant molecules in the folded conformation. In the presence of GuHCl, the intrinsic conformational equilibrium constants (K_1 and K_2) for the two domains of DT are given by expressions similar to eq 6 [$K_1 = K_1^0(1 + k_b a)^{\Delta n_1}$ and $K_2 = K_2^0(1 + k_b a)^{\Delta n_2}$]. These expressions can be substituted into the partition function (eq 1) and through a procedure similar to the one described above obtain the expression for the heat capacity surface as a function of temperature and GuHCl.

Multidimensional Deconvolution. The entire set of DSC data was analyzed simultaneously by using the formalism developed above in conjunction with the GuHCl-dependent conformational equilibrium constants. Global nonlinear least-squares analysis of the heat capacity surface was performed by using both the Marquardt (1963) and the Simplex (Nelder & Mead, 1965) minimization algorithms to find the best unique set of parameters that describe all of the data simultaneously. Table II summarizes the results of the global analysis. The long pretransitional base lines shown in Figure 1 are necessary to statistically uncouple changes in overall ΔH due to GuHCl binding from those due to the ΔC_p for the transition. The solid lines in Figure 1 are the theoretical curves predicted by the parameters in Table II. The standard deviation between the experimental and theoretical curves is 1.7 kcal/(K·mol) over the entire surface. The data are consistent with a GuH^+ association constant of 0.95 M^{-1} at 25 °C which is within the range of 0.1–1.2 M^{-1} found for other proteins in direct GuHCl denaturation studies (Pfeil, 1981). Our results yield a binding enthalpy for GuH^+ of −0.82 kcal/mol which is also close to the value of −2.4 kcal/mol previously estimated by Pfeil and Privalov (1976). Δn values of 20 and 51 GuH^+ binding sites were estimated for the A and B domains, respectively. These numbers are also consistent with values obtained previously for other proteins (Lee & Timasheff, 1974; Pfeil & Privalov, 1976). The ΔC_p values of 3.5 and 4.3 kcal/(K·mol) [0.17 and 0.12 cal/(K·g)] for the A and B do-

mains are of the same magnitude as the value of 0.19 cal/(K·g) estimated previously for the intact toxin (Ramsay et al., 1989). Inspection of the data as a function of GuHCl concentration indicates that the change in cooperative behavior is triggered by a rapid increase in the value of Φ_1 with GuHCl concentration. Whereas at zero GuHCl this quantity is equal to 0.03, it increases to about 0.5 at 0.8 M GuHCl. It was empirically found that Φ_1 can also be represented by an equation similar to eq 7 [$\Phi_1 = \Phi_1^0(1 + k_b a)^{\Delta n}$]. In terms of this formalism, approximately seven or eight previously buried GuHCl binding sites become exposed in the B domain upon unfolding of the A domain. These observations suggest that the cooperative behavior may arise from the unfavorable energy of exposing the hydrophobic domain interface of the partially unfolded states to the aqueous medium. In the presence of GuHCl, this unfavorable free energy diminishes, resulting in the stabilization of the partially unfolded state A_uB_f.

As can be observed in Figure 1, the linked cooperative model accurately predicts the behavior of the system over the entire GuHCl concentration range. The location, areas, and also the shapes of the entire family of calorimetric profiles are reproduced within the limits of experimental error by an unique set of thermodynamic parameters. The advantages of a global analysis like the one performed here over the analysis of each individual curve taken separately reside in the fact that it allows the explicit inclusion of the dependence of the excess heat capacity function on a second independent variable, in this case of GuHCl activity. With this analysis, the entire set of data (about 5000 data points in the experiments presented in this paper) is used to minimize the error surface and obtain the best set of parameters that describe the behavior of the system along the surface defined by the two independent variables, temperature and GuHCl.

Conclusions

The calorimetric data for DT at low GuHCl concentrations clearly show that the thermally induced denaturation of DT is a multistate process. This is consistent with earlier DSC studies of DT as a function of pH and with X-ray crystallography studies which showed the presence of two structural domains (Kantardjieff et al., 1987). Analysis of the data reveals that in the concentration range of 0–0.3 M GuHCl the denaturation can be described in terms of two cooperatively coupled two-state transitions, while in the 0.3–1.0 M range only a single two state-transition is observed. On the basis of studies with the isolated A domain, the low-temperature, low-enthalpy transition was previously assigned to the A domain (Ramsay et al., 1989).

The structural thermodynamic picture of DT that emerges from these studies is that of two interacting domains, with the A domain having a lower intrinsic stability than the B domain. Domain–domain interactions account for most of the structural stability of the A domain under physiological conditions. As the concentration of GuHCl increases over 0.3 M, the A domain progressively becomes unfolded at all temperatures as shown in Figure 6. Under these conditions, the most significantly populated state at temperatures below the transition temperature is the partially unfolded state in which only the B domain retains secondary structure. At GuHCl concentrations higher than 1 M, the completely unfolded state becomes the most significantly populated. The partially unfolded state A_uB_f might be a key intermediate during the membrane translocation process of the A domain. In this conformation, the A domain is unfolded, which appears to be a general requirement during membrane translocation of proteins (Eilers & Schatz, 1987), while the B domain is still able to interact with other membrane components necessary for this process. Our previous calorimetric data obtained as a function of pH (Ramsay et al., 1989) are also consistent with the above mechanism as well as biphasic character of the isothermal pH unfolding profiles previously reported by Blewitt et al. (1985).

Registry No. GuHCl, 50-01-1.

References

Aune, K. C., & Tanford, C. (1969a) *Biochemistry 8*, 4579–4585.

Aune, K. C., & Tanford, C. (1969b) *Biochemistry 8*, 4586–4590.

Biltonen, R. L., & Freire, E. (1978) *CRC Crit. Rev. Biochem. 5*, 85–124.

Blewitt, M. G., Zhao, J. J., McKeever, B., Sarma, R., & London, E. (1984) *Biochem. Biophys. Res. Commun. 120*, 286–290.

Blewitt, M. G., Chung, L. A., & London, E. (1985) *Biochemistry 24*, 5458–5464.

Brandts, J. F., Hu, C. Q., Lin, N. L., & Mass, M. T. (1989) *Biochemistry 28*, 8588–8596.

Castellino, F. J., & Barker, R. (1968) *Biochemistry 7*, 4135–4138.

Cieplak, W., Gaudin, H. M., & Eidels, L. (1987) *J. Biol. Chem. 262*, 13246–13253.

Collier, R. J., & Kandel, J. (1971) *J. Biol. Chem. 246*, 1496–1503.

Creighton, T. E. (1984) in *Proteins: Structure and Molecular Properties*, W. H. Freeman, New York.

DeLange, R. J., Williams, L. C., & Collier, R. J. (1979) *J. Biol. Chem. 254*, 5827–5831.

Drazin, R. E., Collier, R. J., Williams, L. C., & DeLange, R. J. (1979) *J. Biol. Chem. 254*, 5832–5837.

Eilers, M., & Schatz, G. (1987) *EMBO J. 6*, 1073–1077.

Falmagne, P., Capiau, C., Lambotte, P., Zanen, J., Cabiaux, V., & Ruysschaert, J. M. (1985) *Biochim. Biophys. Acta 827*, 45–50.

Freire, E. (1989) *Comments Mol. Cell. Biophys. 6*, 123–140.

Freire, E., & Biltonen, R. L. (1978) *Biopolymers 17*, 463–479.

Ghelis, C., & Yon, J. (1982) in *Protein Folding*, Academic Press, New York.

Hranitzky, K. W., Durham, D. L., Hart, D. A., & Eidels, L. (1985) *Infect. Immun. 49*, 336–343.

Jensen, M. S., & Bainton, D. F. (1973) *J. Cell Biol. 56*, 379–388.

Kantardjieff, K., Dijkstra, B., Westbrook, E. M., Barbieri, J. T., Carrol, S. F., Collier, R. J., & Eisenberg, D. (1987) *UCLA Symp. Mol. Cell. Biol., New Ser. 69*, 187–200.

Lee, J. C., & Timasheff, S. N. (1974) *Biochemistry 13*, 257–265.

Lowry, O. H., Rosebrough, N. H., Farr, A. L., & Randell, R. J. (1951) *J. Biol. Chem. 193*, 265–275.

Marquardt, D. W. (1963) *J. Soc. Ind. Appl. Math. 11*, 431–441.

Masserini, M., & Freire, E. (1987) *Biochemistry 26*, 237–242.

Moskaug, J. O., Sandvig, K., & Olsnes, S. (1987) *J. Biol. Chem. 262*, 10339–10345.

Nelder, J. A., & Mead, R. (1965) *Comput. J. 7*, 308–313.

Ohkuma, S., & Poole, B. (1978) *Proc. Natl. Acad. Sci. U.S.A. 75*, 3327–3331.

Pace, C. N. (1986) *Methods Enzymol. 131*, 266–280.

Pace, C. N., & Vanderburg, K. E. (1979) *Biochemistry 18*, 288–292.

Pfeil, W. (1981) *Mol. Cell. Biochem. 40*, 3–28.

Pfeil, W., & Privalov, P. L. (1976) *Biophys. Chem. 4*, 33–40.

Privalov, P. L. (1979) *Adv. Protein Chem. 33*, 167–241.

Privalov, P. L. (1982) *Adv. Protein Chem. 35*, 1–104.
Privalov, P. L., & Khechinashvili, N. N. (1974) *J. Mol. Biol. 86*, 665–684.
Proia, R. L., Hart, D. A., Holmes, R. K., Holmes, K. V., & Eidels, L. (1979) *Proc. Natl. Acad. Sci. U.S.A. 76*, 685–689.
Ramsay, G., Montgomery, D., Berger, D., & Freire, E. (1989) *Biochemistry 28*, 529–533.
Sandvig, K., & Olsnes, S. (1981) *J. Biol. Chem. 256*, 9068–9076.
Shriver, J. W., & Kamath, U. (1990) *Biochemistry 29*, 2556–2564.
Wyman, J. (1964) *Adv. Protein Chem. 19*, 223–286.
Zhao, J. M., & London, E. (1988) *J. Biol. Chem. 263*, 15369–15377.

Unfolding–Refolding of the Domains in Yeast Phosphoglycerate Kinase: Comparison with the Isolated Engineered Domains†

Dominique Missiakas, Jean-Michel Betton, Philippe Minard, and Jeannine M. Yon*

Laboratoire d'Enzymologie physico-chimique et moléculaire, Groupe de Recherche du Centre National de la Recherche Scientifique associé à l'Université de Paris-Sud, 91405 Orsay, France

Received February 5, 1990; Revised Manuscript Received June 7, 1990

ABSTRACT: The role of domains as folding units was investigated with a two-domain protein, yeast phosphoglycerate kinase. Each of the domains was produced independently by site-directed mutagenesis. It has been previously demonstrated by several criteria that these domains are able to fold in vivo into a quasi-native structure [Minard et al. (1989a) *Protein Eng. 3*, 55–60; Fairbrother et al. (1989) *Protein Eng. 3*, 5–11]. In the present study, the reversibility of the unfolding–refolding process induced by guanidine hydrochloride was investigated for the intact protein and the isolated domains. The transitions were followed by circular dichroism for both domains and the intact protein and by the variations in enzyme activity for the intact protein. Tryptophan residues were used as intrinsic conformational probes of the C-domain. An extrinsic fluorescent probe, *N*-[[(iodoacetyl)amino]ethyl]-8-naphthylamine-1-sulfonic acid (IAEDANS), was bound to the unique cysteinyl residue Cys97 to observe the conformational events in the N-domain. The unfolding–refolding transitions of each domain in the intact protein and in the isolated domains prepared by site-directed mutagenesis were compared. It was shown that the two domains are able to refold in a fully reversible process. A hyperfluorescent intermediate was detected during the folding of both the isolated C-domain and the intact yeast phosphoglycerate kinase. The stability of each isolated domain was found to be similar, the free energy of unfolding being approximately half that of the intact molecule.

The molecular mechanisms by which a polypeptide chain folds into its biologically active three-dimensional structure have been widely investigated by using several different proteins as models. The protein folding process has often been described as a hierarchical succession of structural events (Rose, 1979). At present, the generally accepted model consists of an early stage during which short-range interactions lead to the formation of nucleation centers; then, some stretches of ordered structures are formed that interact to produce new, higher levels of structure, which merge into domains. Finally, the domains associate and interact to generate the native protein (Kim & Baldwin, 1982). It has been proposed that domains are structural entities that are capable of folding independently (Wetlaufer, 1973). Domains, therefore, would constitute the elementary folding units of proteins. Many attempts to demonstrate experimentally the role of domains as kinetic intermediates in the folding pathway of multidomain proteins have been reported. Until now, the only possible approach to studying the behavior of domains during the refolding process has required the isolation of the domains following limited proteolysis or chemical cleavage [see Wetlaufer (1981), Ghélis and Yon (1982), and Jaenicke (1987) for reviews].

Phosphoglycerate kinase is a good model for the study of domain folding. The three-dimensional structures of horse muscle (Banks et al., 1979) and yeast (Watson et al., 1982) phosphoglycerate kinases, both monomeric enzymes, have revealed two globular units corresponding to the amino- and carboxyl-terminal halves of the molecules called the N- and C-domains, respectively. The C-domain, which binds nucleotide substrates, contains a Rossmann fold. The study of the unfolding–refolding transition at equilibrium of the horse muscle phosphoglycerate kinase, using different conformational probes (Betton et al., 1984), has suggested that the domains refold independently and that the C-domain is more stable. Kinetic data have confirmed the presence of an intermediate in which the C-domain is partially or totally folded (Betton et al., 1985). Limited proteolysis of this enzyme, using conditions under which the folding intermediates are more populated, has given a stable fragment identified as the C-terminal part of the protein (Betton et al., 1989). This fragment has been found to be partially folded, supporting the conclusion that the C-domain might be a folding unit. Adams et al. (1985) have obtained a fragment corresponding to a part of

† This work was sponsored by the Centre National de la Recherche Scientifique, the Ministère de la Recherche et de la Technologie (Grant 635), the Fondation pour la Recherche Médicale Française, and a contract with the Centre National de Transfusion Sanguine.
* To whom correspondence should be addressed.

0006-2960/90/0429-8683$02.50/0